Deformation behaviour of SCP improved ground to limit state

Comportement en déformation à l'état limite d'un sol amélioré par SCP

H. Takahashi & M. Kitazume
Port and Airport Research Institute, Yokosuka

K. Maruyama
GeoDesign, Tokyo

ABSTRACT

The sand compaction pile (SCP) method has been used in many construction sites to improve soft clay layers. Clay ground improved by the SCP method can be assumed as a composite of sand compacted piles and a soft clay layer. This type of composite ground shows complicated deformation and failure patterns under backfill loading because of the different characteristics of the component materials. The stability of SCP improved ground has been studied under the assumption of shear strength on a slip surface. However, for performance design by checking displacement, it is essential to appropriately calculate the deformation and failure behaviour of improved ground subjected to the limit state. In this study, some SCP improved grounds were subjected to centrifuge model tests to investigate the deformation and failure patterns. Then, a finite element analysis based on the elasto-viscoplastic constitutive equation was applied to the model tests, and the calculation accuracy of numerical analysis was assessed. Finally, the mechanism of failure of the SCP improved ground subjected to the limit state was investigated. The model tests indicated that the low replacement SCP improved ground did not fail with the sliding mode but with the bending mode. Moreover, the calculation accuracy of FEM analyses was confirmed, and the drainage of the clay layer between sand walls restrained the sharp increase in ground deformation.

RÉSUMÉ

La méthode des pieux de sable compactés (SCP) a été utilisée dans de nombreux chantiers afin d'améliorer des couches d'argiles molles. Un sol argileux amélioré par la méthode SCP est un sol composite consistant de pieux de sable compactés et d'une couche d'argile molle. Lorsqu'il est soumis à une charge en remblai, ce type de sol composite présente un comportement complexe en déformation et à la rupture, en raison des caractéristiques différentes des matériaux qui le composent. La stabilité d'un sol amélioré par SCP a été étudiée en faisant l'hypothèse d'une résistance au cisaillement le long d'une surface de glissement. Cependant, pour une approche de conception basée sur la performance, qui utilise les déplacements comme critère, il est essentiel de déterminer de manière adéquate le comportement en déformation et en rupture des sols améliorés soumis à l'état limite. Dans cette étude, des sols améliorés par SCP ont été soumis à des essais modèles en centrifuge afin d'analyser les caractéristiques principales du comportement en déformation et à la rupture. Ensuite, une analyse aux éléments finis basée sur l'équation constitutive élasto-viscoplastique a été appliquée aux essais modèles, et la précision de calcul de l'analyse numérique a été évaluée. Finalement, le méchanisme de rupture du sol amélioré par SCP soumis à l'état limite a été examiné. Sur la base des esssais modèles, il a été conclu que le sol amélioré par SCP à remplacement faible n'atteint pas la rupture en mode de glissement, mais atteint la rupture en mode de flexion. De plus, la précision de calcul des analyses FEM a été confirmée, et le drainage de la couche de sable entre des murs sableux a restreint une brusque augmentation de déformation du sol.

Keywords : sand compaction pile method, centrifuge model test, finite element method, backfill loading

1 INTRODUCTION

The sand compaction pile (SCP) method has been used in many construction sites to improve soft clay layers. SCP is a typical ground improvement method, where a casing pipe is used to install compacted sand piles in a clay layer to increase the ground strength and improve drainage performance. SCP is one of the most commonly used methods in Japan. Recycled or man-made materials are often used instead of sand, and SCP will be the main method for ground improvement at such sites. SCP is also used for many gravity-type quays to increase stability for backfill loading. This study was performed to characterise the deformation of SCP improved ground under backfill loading.

Clay ground improved by the SCP method can be assumed as a composite of compacted sand piles and a soft clay layer. This type of composite ground shows complicated deformation and failure patterns under backfill loading because its component materials have different characteristics. The stability of SCP improved ground has been studied under the assumption of shear strength on a slip surface. Many studies were performed using stability assessment methods which assumed a slip failure, and this is included in the current design method. Although there have been few investigations of the failure properties of SCP improved ground under backfill loading, some studies examined the failure patterns of improved ground under fill loading. For example, Almeida *et al.* (1985), Takemura *et al.* (1991) and Ng *et al.* (1998) performed centrifuge model tests to determine the failure patterns of SCP improved ground. In addition, there have been a number of recent studies of the deformation characteristics of improved ground. Rahman *et al.* (2000) and Mizuno *et al.* (2007) investigated the deformation of improved ground under backfill loading. However, these studies were performed to determine ground deformation during consolidation after stable backfilling, and the deformation properties of ground subjected to the limit state were not investigated. For performance design by checking displacement, it is essential to appropriately calculate the amount of deformation of ground subjected to the limit state.

In this study, some SCP improved grounds were subjected to centrifuge model tests to investigate the deformation and failure patterns. Then, a finite element analysis based on the elasto-viscoplastic constitutive equation was applied to model tests, and the accuracy of numerical analysis was assessed. Finally, the mechanism of failure of the SCP improved ground subjected to the limit state was investigated.

Proceedings of the 17th International Conference on Soil Mechanics and Geotechnical Engineering
M. Hamza et al. (Eds.)

doi:10.3233/978-1-60750-031-5-2272

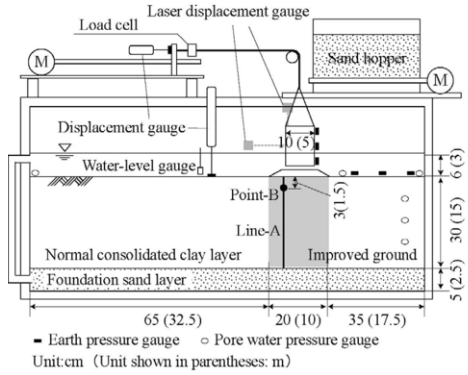

Figure 1. Schematic view of model ground

Table 1. List of centrifuge model test cases

Case	Diameter of piles	Replacement ratio	Mass of caisson	Limit backfill pressure
SCP181	2 cm	28 %	2.70 kg	53 kN/m^2
SCP182	2 cm	11 %	1.38 kg	44 kN/m^2
SCP183	4 cm	28 %	2.70 kg	53 kN/m^2

2 CENTRIFUGE MODEL TESTS

2.1 *Overview of preparation and procedure of model tests*

Many centrifuge model tests have been carried out on many geotechnical subjects to investigate full-scale ground behaviour, in which a small-scaled model ground is subjected to high centrifugal acceleration. Figure 1 shows a schematic view of the model ground and loading apparatus. A rigid specimen box is rectangular box with internal dimensions of 120 cm (length) × 20 cm (width) × 60 cm (height).

The clay ground material investigated in this study was a mixture of MC kaolin clay and AX kaolin clay (50% and 50%). The de-aired kaolin clay with a water content of 120% was poured on the base sand layer and was preliminarily consolidated on the laboratory floor by bellowphragm cylinders. After completion of the preliminary consolidation, the model ground was brought up to a centrifugal acceleration of 50G and allowed to consolidate by enhanced self-weight. In this study, compacted sand piles with a diameter of 2 or 4 cm were made in an acrylic pipe, the relative density of which was about 75%. The sand pile in the pipe was frozen for ease of installation into the ground. Small holes were excavated in the clay ground, and sand piles in a frozen condition were installed in a rectangular arrangement, with a replacement ratio a_s of 11 or 28%. Three model test cases are summarised in Table 1.

After embedding several pore water pressure gauges and earth pressure gauges in the model ground, a sand hopper for sand filling and a lift for a model caisson were installed on the specimen box. The model ground thus prepared was brought up to a centrifugal acceleration of 50G for self-weight consolidation. After consolidation the model caisson was put on the sand mound, and after 60 s later the backfilling was constructed by sand raining from the sand hopper. Backfilling was carried out in a stepwise manner at a height increase of 1 cm per 5 s followed by a pause of 25 s.

2.2 *Results of model tests*

2.2.1 *Ground displacement and backfill pressure*

Figure 2 shows the relationship between the ground horizontal displacement and the backfill pressure, which were measured in each test case. The vertical axis represents the horizontal displacement measured at point-B as shown in Fig. 1. The backfill pressure on the horizontal axis was the vertical effective

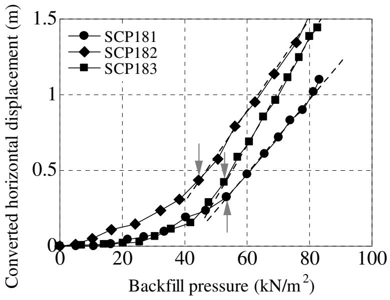

Figure 2. Relation between ground displacement and backfill pressure

earth pressure from the backfill layer. In all test cases, the horizontal displacement increased when the improved ground was subjected to larger backfill pressure. The displacement in SCP182, the replacement ratio a_s of 11%, was larger than those in SCP181 and 183 in the early stage of backfill loading. This would be because the mean stiffness of the improved area of SCP182 of the low replacement was smaller than those of the other test cases. In addition, the exponential increase of horizontal displacement in SCP182 can be observed in the early stage. This indicated that the comprehensive strength in SCP182 was also the smallest. By comparing the measured data in SCP181 and 183, which had the same replacement ratio but not the same diameter of the sand pile, the horizontal displacements in these test cases were almost the same below the backfill pressure of 50 kN/m^2. The both relationship between displacement and pressure showed a steep increase around the backfill pressure of 50 kN/m^2. This pressure indicated the yield stress. After the backfill pressure exceeded the yield stress, the displacement increased linearly for the backfill pressure. It should be noted that the displacement in SCP183 above 50 kN/m^2 increased more rapidly than that in SCP181. Thus, the ratio of the strength increase of improved ground in SCP183 was larger than that in SCP181.

As shown in Fig. 2, the relationship between horizontal displacement and backfill pressure had no peak value, and the limit points of ground were not obtained explicitly. For this reason, the starting point of the last line of the relationship was defined as a limit point of improved ground. The last linear relation indicated no alteration in the ground failure mode, and the ground already reached the limit state. The backfill pressure of the starting point of the last line is defined as a limit backfill pressure. The limit backfill pressure is an index for assessing the ground stability. Table 1 includes the limit backfill pressure of each test case. By comparing the limit backfill pressures in SCP181 and 182, the limit pressure in SCP182 was 17% smaller than that in SCP181 due to the low replacement ratio in SCP182. The limit backfill pressures in SCP181 and 183 resulted in the same value of 53 kN/m^2. These test results indicated that the diameter of sand piles did not influence the comprehensive strength of improved ground but the rate of increase in strength after yield stress.

2.2.2 *Deformation mode of improved ground*

Figure 3 shows the distribution of horizontal displacement along Line-A, which is shown in Fig.1. The distributions in SCP181 and 183, the replacement ratio a_s of 28%, showed the maximum value of 5 cm in the prototype scale under the backfill pressure of about 30 kN/m^2. The maximum displacement in SCP182, the replacement ratio a_s of 11%, approached 12 cm under the same backfill pressure. The magnitude of the displacements decreased gradually with depth regardless of the replacement ratio. When the backfill pressure exceeded 60 kN/m^2, the improved portion displaced horizontally, like dropping toward the sea, and bent almost at the mid-depth.

Figure 4 shows a cross-sectional view of the improved ground taken after the model test. The test case is SCP182. As shown in this photograph, all sand piles deformed toward to the

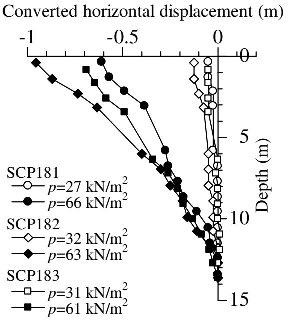

Figure 3. Distribution of horizontal displacement of improved ground

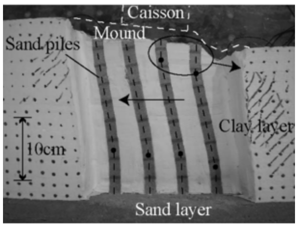

Figure 4. Cross-sectional view of improved ground after loading test

sea side with bending deformation. The sand piles had a curvature factor of over 2 m^{-1} on the photograph, and the curvature of 2 m^{-1} corresponded to the axial strain of over 2% on the lateral edge of the sand pile. This strain level indicated that the edge of the sand pile reached the plastic range. On the other hand, the clay layer between sand piles showed uniform shearing, and the maximum shear strain exceeded 20%. The clay layer fully failed. Thus, the low replacement SCP improved ground did not fail with the sliding mode but failed with the bending mode. SCP improved ground under the limit state showed resistance to backfill loading with the bending mode, where sand piles bent and the clay layer between sand piles sheared. In addition, the upper portion of the sand pile located at the backfill side was deformed toward the backfill side, as shown in Fig. 4. This was due to the consolidation of the clay ground under the backfill layer. Although the photographs of other test cases are not shown, the same deformation behaviour, such as the bending mode, was observed in other test cases.

3 NUMERICAL ANALYSIS

3.1 *Program and modeling of finite element method*

The FEM program GeoFem, which has been applied to many construction projects of port and offshore airport facilities in Japan, was used for numerical analyses (Kobayashi, 1984). The program uses an elasto-viscoplastic algorithm under the fluid-soil interaction. The elasto-viscoplastic model followed the model proposed by Sekiguchi and Ohta (1977). The original model of Sekiguchi and Ohta calculates large horizontal displacement for the caisson under backfill loading. The target model of this paper was also the caisson and ground under backfill loading, and the horizontal displacement was probably overestimated. Therefore, the yield surface of the modified Cam-clay model was applied to FEM analysis, because the yield surface of the modified Cam-clay model is of the elliptic type and can reduce shear strain and horizontal displacement (Mizuno *et al.*, 2007).

On a practical level, the ground improved by sand piles is frequently modelled by an uniform solid with larger stiffness and strength than the clay layer. This modelling method for SCP improved ground is mainly used for simulating the ground deformation within the ground stability. However, the uniform solid model cannot simulate the bending mode of sand piles, which was observed in the centrifuge model tests. Therefore, a modelling method as a wall type improved ground was adapted

Table 2. Soil parameters used for FEM analysis

(a) Clay layer

λ	κ	ν'	γ' (kN/m^3)	e_0
0.195	0.039	0.38	6.3	1.7

M	K_0	α	$\dot{v}_0$ (1/day)	k (m/day)
0.91	0.61	0.0025	1.0×10^{-4}	7.94×10^{-4}

(b) Other materials

	E' (MN/m^2)	ν'	γ' (kN/m^3)	ϕ' (Degree)
Caisson	1000.0	0.17	4.7	-
Backfill layer	2.9	0.31	Step-up	33.0
Sand mound	6.9	0.31	9.3	33.0
Sand wall	19.6	0.33	9.5	42.0

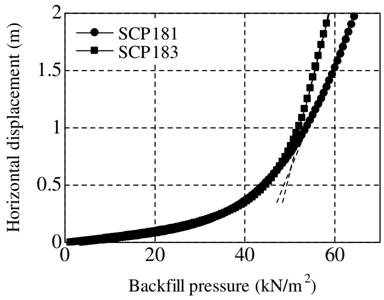

Figure 5. Calculated ground displacement and backfill pressure

for the numerical analyses. The improved ground modelled consisted of the sand walls and the clay walls with improvement area ratios of 28% or 11% as in the model tests.

The scale in the FEM analysis was converted to a prototype scale by multiplying the centrifugal acceleration. The soil parameters of the clay layer and some materials are summarised in Table 2. The model caisson was modelled as a linear elastic solid, and the backfill layer, the sand mound and sand walls simulating sand compaction piles, were modelled as an elastic-perfectly plastic solid with Mohr-Coulomb's failure criteria. The clay layer was modelled as an elasto-viscoplastic solid, and the compression index λ, swelling index κ and permeability coefficient k were obtained by the consolidation test. The K_0-value, Poisson ratio ν', Shear strength M were determined by the consolidated undrained triaxial test.

3.2 *Comparison between numerical analysis and model test*

The relationship between the horizontal displacement just beneath the sand mound and the backfill pressure, which were calculated by FEM analyses, is shown in Fig. 5. FEM analyses were conducted to simulate SCP181 and 183. The vertical and horizontal axes show the horizontal displacement and the backfill pressure, respectively. The displacement calculated linearly increased for the backfill pressure in the early stage of loading, regardless of the thickness of the sand wall. The displacement increased nonlinearly when the improved ground was subjected to large backfill pressure. The relationship between the horizontal displacement and the backfill pressure in the last stage of loading was linear in the graph, and the line had a finite gradient. This behaviour simulated by the FEM analyses agreed rather well with that in the model test. The linear gradients in SCP181 and 183 were almost the same in the early stage, but those in last stage were different. The relations of the gradients agreed with those observed in the model tests. SCP181 and 183 had the same replacement ratio and a different interval between sand walls, and the drainage distance of the clay layer between sand walls in SCP183 was larger than that in SCP181. This difference in drainage distance was considered to have a marked effect on the gradient of the last line. The details are given in the next section.

Based on the relationship between the displacement and the backfill pressure shown in Fig. 5, the limit backfill pressures

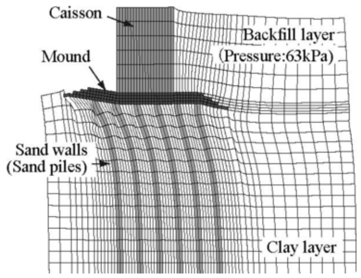

Figure 6. Calculated ground deformation under the limit state

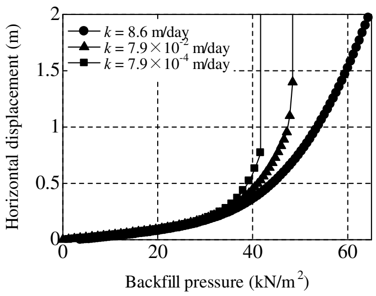

Figure 7. Calculated displacements by changing the drainage rate

were obtained according to the definition used in the model test. The limit backfill pressures in SCP181 and 183, of which the thicknesses of the sand wall were 0.5 and 1.0 m, were the same (51 kN/m^2). The calculated limit backfill pressure of 51 kN/m^2 was close to that of the model test, and the calculation accuracy for the ground stability was high.

Figure 6 shows the calculated ground deformation under the limit state defined by the backfill load and the displacement relation. The caisson, sand mound, and sand walls are coloured to make it easier to distinguish the ground deformation. The sand walls bent almost at the mid-depth and the clay between the sand walls was markedly sheared. In the FEM analysis, the improved ground did not fail with the sliding mode but failed with the bending mode as in the model test. The FEM analysis could also simulate that the upper portion of the sand pile located at the backfill side deformed toward the backfill side. Thus, the FEM analyses performed in this study was confirmed to have high calculation accuracy in ground deformation.

3.3 *Parametric study by numerical analysis*

As indicated above, the relation between the displacement and backfill pressure had a finite gradient even under the limit state. The finite gradient of the last line indicated that the strength of improved ground for the backfill loading increased during backfill loading. The increase in strength of improved ground would be due to drainage of the clay layer between sand walls. Therefore, the larger gradient of the last line in SCP183, in which the drainage of the clay layer was greater than that in SCP181, can be easily understood. To confirm the effects of drainage of the clay layer between sand walls, some additional FEM analyses were parametrically conducted to change the permeability coefficient of the sand walls. However, the change in permeability of sand walls had a marked effect on the shear strength, because the shear strength of the sand was given by the internal friction angle ϕ. To remove the effect of the differences in shear strength of the sand walls, the shear strength of sand was virtually provided from the adhesive strength c.

Figure 7 shows the calculated horizontal displacement and the backfill pressure by changing the drainage rate of the clay layer between the sand walls. In the case where the drainage rate was low, the horizontal displacement started to increase early, and the relation between the displacement and backfill pressure showed a sharp incline. To increase the drainage rate, the gradient of the last line decreased in the graph. In cases in which the drainage rate was low, the shear strength of the clay layer between the sand walls did not increase during backfill loading, and a large shear strain occurred in the clay layer. The large shear strain generated large horizontal displacement. Thus, the stability of SCP improved ground can be increased by rapid draining the excess pore water pressure generated in the clay layer between sand piles under backfill loading. In addition, the sharp increase of ground deformation under the limit state can be also restrained when the drainage rate of clay layer is high.

4 CONCLUSIONS

In this study, a clay ground improved by sand piles were subjected to centrifuge model tests to investigate the deformation and failure patterns. Then, a finite element analysis based on the elasto-viscoplastic constitutive equation was applied to the model tests, and the accuracy of the numerical analysis was verified. Finally, the mechanism of failure of the improved ground subjected to the limit state was investigated. The major conclusions derived can be summarised as follows:

1) The displacement of the SCP improved ground increased nonlinearly when the improved ground was subjected to the backfill loading. However, the relationship between displacement and backfill pressure in the last stage of loading was linear. If the starting point of the last line of the relationship was defined as a limit point, the limit backfill pressure of the improved ground of a_s = 11% was 17% smaller than that of a_s = 28%. Meanwhile, the diameter of sand piles had negligible effect on the ground stability.

2) The ground deformations under backfill loading and the cross-sectional view of the improved ground after the model test indicated that the sand piles deformed toward the sea side with bending deformation. The low replacement SCP improved ground did not fail with the sliding mode but failed with the bending mode.

3) The FEM analyses using the modified Sekiguchi and Ohta model were performed to investigate the deformation and the failure behaviour of the improved ground. It was confirmed that the calculation accuracy was high. Moreover, drainage of the clay layer between the sand walls restrained the sharp increase in ground deformation because the shear strength of the clay layer was increased. This knowledge regarding to the deformation behaviour of improved ground is important for good performance design by checking displacement.

REFERENCES

Almeida, M.S.S., Davis, M.C.R. & Parry, R.H.G. 1985. Centrifuge Tests of Embankments on Strengthened and Unstrengthened Clay Foundations. *Geotechnique* 35, No. 4: 425-441.

Kobayashi, M. 1984. Stability Analysis of Geotechnical Structures by Finit Elements. *Report of the Port and Harbour Research Institute* 23, No. 1: 83-101. (in Japanese)

Mizuno, K., Tsuchida, T., Kobayashi, M. & Watabe, Y. 2007. New Constitutive Equation of Clay and the Prediction of Horizontal Deformations of Large Scale Embankments. *JSCE Journal* C/63, No. 4: 936-953. (in Japanese)

Ng, Y.W., Lee, F.H. & Yong, K.Y. 1998. Development of an In-flight Sand Compaction Piles (SCPs) Instraller. *Proceedings of the Centrifuge 98*, Tokyo, Japan: 837-843.

Rahman, Z., Takemura, J., Kouda, M. & Yasumoto, K. 2000. Experimental Study on Deformation of Soft Clay Improved by Law Replacement Ratio SCP under Backfilled Caisson Loading. *Soils and Foundations* 40, No. 5: 19-35.

Sekiguchi, H. & Ohta, H. 1977. Induced Anisotropy and Time Dependency in Clays. *Specialty Session 9; Proceedings of the 9th ICSMFE*: 229-238.

Takemura, J., Tean, L.B., Suemasa, N., Hirooka, A. & Kimura, T. 1991. Stability of Soft Clay Improved with Sand Compaction Piles under a Fill. *Proceedings of the GEO-COAST 91*, Yokohama, Japan: 399-404.